Available online at www.sciencedirect.com
SCIENCE DIRECT®
Journal of Photochemistry and Photobiology A: Chemistry 156 (2003) 161–170
Journal of Photochemistry and Photobiology A:Chemistry
www.elsevier.com/locate/jphotochem

TiO_2 photocatalytic oxidation of nitric oxide: transient behavior and reaction kinetics

Sid Devahasdin, Chiun Fan, Jr., Kuyen Li, Daniel H. Chen*

Department of Chemical Engineering, Lamar University, Beaumont, TX 77710, USA

Received 6 March 2002; received in revised form 15 December 2002; accepted 17 December 2002

Abstract

Photocatalytic oxidation (PCO) of nitric oxide (NO) over TiO_2 catalyst was studied at source levels (5–60 ppm). The PCO process involves a series of oxidation steps by the $OH^•$ radical: $NO \rightarrow HNO_2 \rightarrow NO_2 \rightarrow HNO_3$. The product NO_2 can be collected in an adsorbent bed and either recycled back to the combustion chamber or recovered as nitric acid. The ratio of NO_2^- to NO_3^- from spent catalyst liquor drops with irradiation time until a steady state is reached. The reactions are limited by thermodynamic equilibrium after ~12 s space time. The steady-state experimental data from space time and inlet concentration effects can be described with the Langmuir–Hinshelwood (L–H) kinetic model with $R^2 = 0.9208$.

Keywords: Photocatalytic oxidation; Nitrogen oxides; Air pollution; Titanium dioxide; Reaction kinetics; Transient behavior

1. Introduction

Nitrogen oxides (NO_x) generally refer only to the major species: nitric oxide (NO) and nitrogen dioxide (NO_2) in air pollution control. NO_x is responsible for tropospheric ozone/particulate (urban smog) through photochemical reactions with hydrocarbon. Further, NO_x together with SO_x (sulfur dioxide and sulfur trioxide) is the major contributor to the "acid rain" that harms forest and crops, as well as aquatic life [1–3]. Thus, NO_x emission has been a focus of environmental regulations, especially in the ozone non-attainment areas.

Reactive nitrogen, denoted NO_y, is defined as the sum of the two oxides of nitrogen ($NO_x = NO + NO_2$) and all compounds that are products of the atmospheric oxidation of NO_x. These include nitric acid (HNO_3), nitrous acid (HNO_2), nitrate radical (NO_3), dinitrogen pentoxide (N_2O_5), peroxynitric acid (HNO_4), peroxyacetyl nitrate (PAN) ($CH_3C(O)OONO_2$) and its homologues, peroxyalkyl nitrates ($RC(O)OONO_2$). Such compounds may be labile via photolysis (e.g. HNO_2) or thermal decomposition (e.g. PAN) and can be regarded as reservoirs for NO_2. However, they do not play the same critical role that NO_2 and NO do as O_3 precursors [2,4].

Currently, the NO_x control technologies include combustion modifications, dry processes, and wet processes. The combustion modification technologies, such as gas reburning, flue gas recirculation, diluent injection, and low NO_x burners, are considered to be suitable for operations with single-digit NO_x emission levels [5]. Dry processes include selective catalytic/non-catalytic reduction (SCR/SNCR) of NO_x to N_2 with ammonia, urea, and hydrocarbons, non-selective catalytic reduction (NSCR) of NO_x to N_2 with H_2, CO, and hydrocarbons, and adsorption [6]. Wet processes include absorption with liquid phase oxidation, absorption with liquid phase reduction, and gas phase oxidation followed by absorption. Among the above-mentioned NO_x emission control technologies, the combustion modification (e.g. low NO_x burners) and SCR are the most popular [6–8]. Alternate NO_x oxidation technologies with O_3, H_2O_2, or electron beam can also achieve nitrogen fixation, but require high energy [3].

2. Photocatalytic oxidation (PCO)

PCO has gained much attention in the purification of air and water because it provides an attractive alternative to the more conventional methods such as carbon adsorption, incineration, and catalytic oxidation. PCO employs semiconductors such as $SrTiO_3$, TiO_2, ZnO, ZnS, and CdS as a photocatalyst [9,10]. Titanium dioxide (TiO_2), which

* Corresponding author. Tel.: +1-409-880-8786; fax: +1-409-880-2197.
E-mail address: chendh@hal.lamar.edu (D.H. Chen).

1010-6030/03/$ – see front matter © 2003 Elsevier Science B.V. All rights reserved.
doi:10.1016/S1010-6030(03)00005-4

has a band gap of 3.2 eV, is most widely used. With TiO_2, the chemical activation is provided by UV (<387 nm) to generate electron–hole (e^-–h^+) pairs. Holes are trapped by the OH^- ions or H_2O present on the surfaces and electrons reduce the adsorbed oxygen yielding highly oxidative hydroxyl radical ($OH^\bullet$), hydroperoxide radical ($HO_2^\bullet$), and superoxide ion ($O_2^{\bullet -}$), which are responsible for the oxidative attacks [10–12]. In the water treatment, PCO has been applied to treat water contaminated with TCE, MEBE, dye, cyanide, and metals. In the purification of air, PCO has found applications in dry cleaning, surface coating, photo processing, process vent treatment, soil vapor extraction, air stripping, and indoor air purification [13,14]. PCO is shown to be more cost-effective than incineration, carbon adsorption, and bio-filtration for flow rates up to 20,000 cfm (ft^3/min) for treating a 500 ppm VOC-laden stream [14].

PCO offers the following distinctive advantages when compared to competing technologies: (1) ability to oxidize low-concentration and low-flow rate waste streams at, but not limited to, ambient temperatures and pressures; (2) ease of operation (instant on/off), modularity, and portability; (3) complete mineralization for hydrocarbons; (4) by-products amenable to bio-remediation for oxygenates [15,16]; (5) potential utilization of solar energy with semiconductor particles (e.g. TiO_2) with a mechanism similar to that of photosynthesis in green plants [17].

2.1. PCO of NO_x-nitrogen fixation

As of today, most of the PCO applications involve the mineralization of VOCs to CO_2, water, and chloride. In Japan, PCO also has been applied to remove ambient NO by coating TiO_2 on the walls of traffic tunnels, paved roads, and buildings [18]. Along this line, the applications also include indoor air cleaners and car deodorizers where indoor VOCs are oxidized over TiO_2 activated by sunlight or fluorescent light [10,17,19]. Ibusuki and Takeuchi [18], Suzuki [19], and Negishi et al. [20] all mixed activated carbon with TiO_2 to adsorb the pollutants and intermediates. Anpo [17] reported that visible light irradiation of metal-implanted TiO_2 leads to significant photocatalytic reactions, including the reduction of NO.

The present paper deals with PCO of NO in source levels (5–60 ppm). The oxidation yields nitric acid and nitrogen dioxide (NO_2). The latter can be collected in an adsorbent bed (e.g. activated carbon and Na-Y zeolite) and either recycled back to the combustion chamber or recovered as nitric acid [7,20,21]. In our view, photocatalytic oxidation of NO_x offers the following distinctive advantages: (1) no extra reactants such as NH_3 or O_3 required; (2) NO_x recycled or recovered as nitric acid, a potential raw material for fertilizers.

While the most popular NO_x control methodology is to reduce NO_x back to N_2, another approach is to oxidize NO to NO_2 and HNO_3 along the general direction of nitrogen fixation. The combustion process that generates NO_x is part of the fixation process but does not go far enough. Further oxidation to nitric acid (HNO_3) will complete nitrogen fixation and become beneficial. As the availability of nitrogen fertilizer is almost always the limiting factor in crop productivity, the nitrogen fixation process is quite desirable [22].

In this study, nitric oxide, the major component of NO_x, was photocatalytically oxidized over titanium dioxide catalyst. The transient behavior of photocatalytic oxidation of NO, oxidation products, and effects of catalyst weight, space time, inlet concentration, humidity, and light intensity were examined. All steady-state kinetic data were analyzed and fitted into the Langmuir–Hinshelwood (L–H) model, and a reaction mechanism is proposed for the PCO of NO.

3. Results and discussion

The experimental setup—including the gas supply, reactor, and analytical system—is shown in Fig. 1. One stream of air bubbled through a gas wash bottle, which contained water. By varying the flow rate of this stream, the humidity can be adjusted. The air, NO, and N_2 streams were mixed to obtain the desired concentration and to adjust space time. Space time is defined as the reactor volume divided by the gas flow rate and is also known as residence time or retention time.

NO was oxidized using a thin-film photoreactor coated with TiO_2. The P-25 TiO_2 powder (Degussa) was 70% anatase. The Pyrex reactor was irradiated with two 8 or 25 W black lights (GE, F8T5-BL or F25T8-BL) from both sides. The light intensity of the 25 W bulbs was varied with a dimming electronic ballast. The reactor setup and light sources were set in an insulated chamber, which could control temperature. The light intensity was measured with the UVA radiometer (Extech Instrument, Model 40736A) in the range of 320–390 nm. The radiometer was placed inside the reactor, and the average of 10 light intensity readings was taken at each input voltage. NO and NO_2 were measured with Thermo Environmental Model 10S chemiluminescent NO–NO_x gas analyzer. The NO gases (28.5, 472 ppm) were purchased from Air Liquide. Used catalyst was scrubbed with de-ionized water, and the liquor was injected into an Alltech 490101 Universal Ion Chromatography System for analyzing NO_2^- and NO_3^-.

TiO_2 (500 mg) was first mixed with 20 ml de-ionized water to make slurry. The cleaned inner tube was placed in the oven (300 °C) for 6 min. The tube was then brush-coated with the catalyst slurry for nine times. The heating and brushing process was repeated until the desired catalyst weight was obtained. It was found that a catalyst loading >0.7 mg/cm^2 did not further increase the conversion of NO. A typical catalyst loading was 1.0 mg/cm^2.

Blank tests (with black lights turned on but without TiO_2) using 20–200 ppm inlet NO with the presence of 0–20% oxygen did not show any NO photolysis at room temperatures. There was also no NO_2 observed when black lights were turned-off and TiO_2 catalyst was present in the reactor.

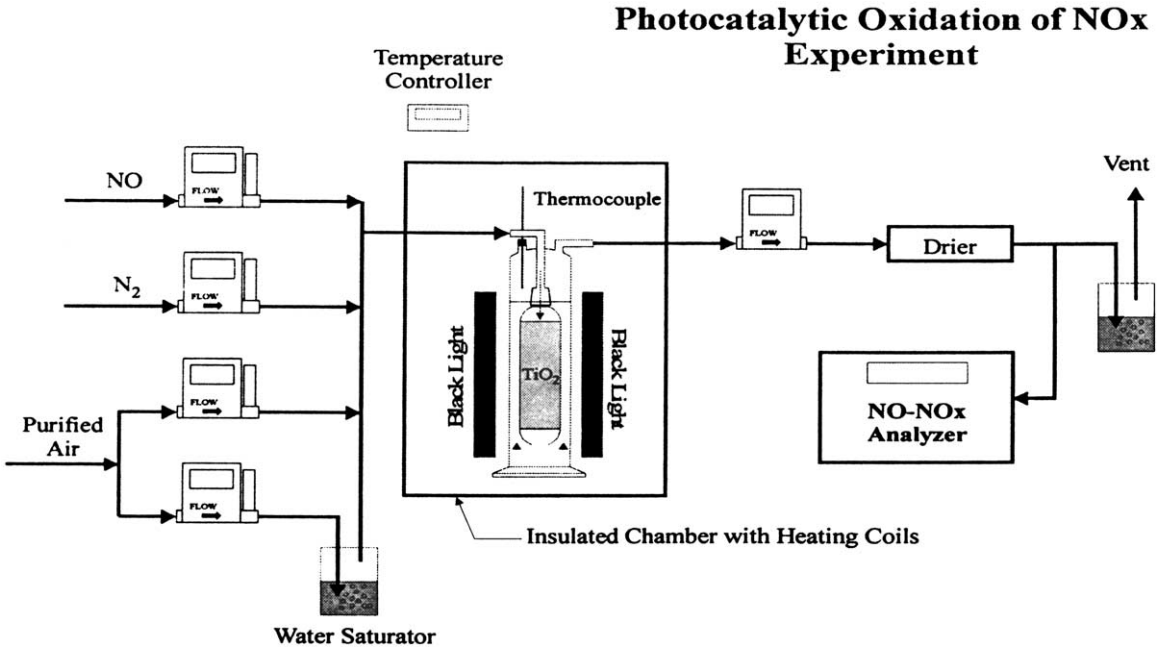

Fig. 1. Experiment setup.

3.1. Transient behavior

At the beginning, a very high conversion was observed. The initial high conversion then decreased and approached a steady state after hours of operation, Figs. 2 and 3. The initial high conversion is believed to come from the high initial rate of adsorption plus reaction (chemisorption) of NO. The time to steady state increased with the amount of catalyst coated [23,24]. The highest conversion reached approximately 95% at 0.5–3 min irradiation time depending on the catalyst loading. Note that the steady state is achieved after around 6 h of irradiation and all the nitrogen is accounted for in the gas phase: NO out (26 ppm) + NO_2 out (14 ppm) = NO in (40 ppm), Fig. 3. The conversion of NO is 35%. The gas phase mass balance indicates that there is no N_2O produced in our reaction system at steady state.

3.2. Inlet concentration/space time effect

At the steady state (with average catalyst loading of 1 mg/cm^2), a lower initial concentration yields a higher conversion, Fig. 4. A longer space time leads to a higher

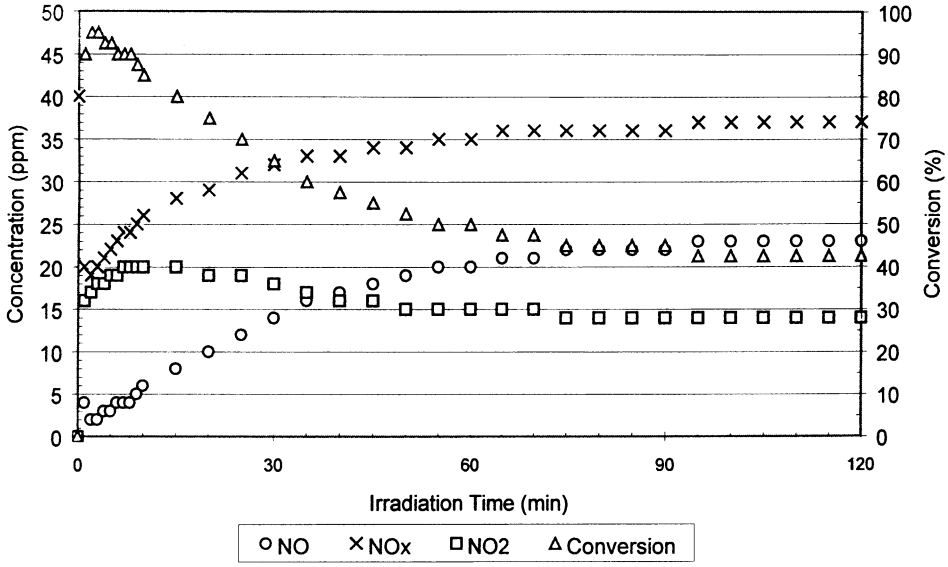

Fig. 2. Transient behavior of the catalyst during the first 2 h of operation (space time: 12 s, inlet concentration: 40 ppm, light source: 2 × 8 W BL; relative humidity: 50%; catalyst weight: 1.07 mg/cm^2).

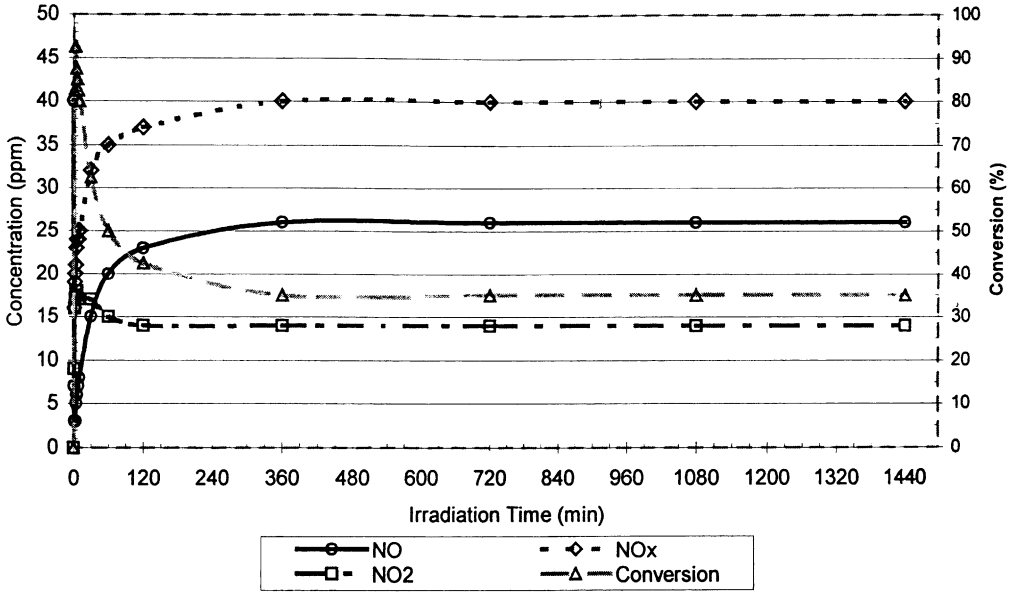

Fig. 3. Long-term behavior of the catalyst (all concentrations are measured in the effluent, space time: 12 s, inlet NO concentration: 40 ppm, light source: 2 × 8 W BL, relative humidity: 50%, catalyst weight: 1.11 mg/cm^2).

conversion until the space time is 12 s, after which the conversion remains constant. This phenomenon indicates that the PCO is limited by equilibrium after 12 s space time. With the same space time, a lower initial concentration gives rise to a higher conversion.

Fig. 5 indicates that the NO_2 selectivity increases at low inlet concentrations and then reaches a plateau once the inlet concentration is higher than 10 ppm. The NO_2 selectivity, however, remains steady at 100% versus space time from 2 to 24 s. NO_2 selectivity is defined as the percent of converted NO that yields NO_2.

Fan [25] reported the NO conversion versus gas flow rate at constant space time of 9.2 s, Fig. 6. The NO conversion was kinetics limited rather than external-mass-transfer limited when flow rates were greater than 0.4 l/min. This was the same flow rate range used in this study.

3.3. Light intensity effect

The light intensity was varied as described in the experimental section. NO conversion and NO_2 selectivity were measured at the steady state (approximately 18–24 h of irradiation time). The NO conversion increases with light intensity. At 5 ppm, NO conversion changes only a little from 0.2 to 0.8 mW/cm^2 corresponding to 12.5–50 W. At 40 ppm, the rate of NO conversion increases steadily from 0.2 to 0.8 mW/cm^2. It is possible that at 5 ppm, the NO conversion is limited by the amount of NO adsorbed on the active sites while at 40 ppm the limiting factor shifts to available UV light, Fig. 7.

Fig. 8 shows the NO_2 selectivity remains constant at 100% for 40 ppm inlet NO and increases with light intensity for 5 ppm inlet NO with a 50% RH. Therefore, for 40 ppm inlet

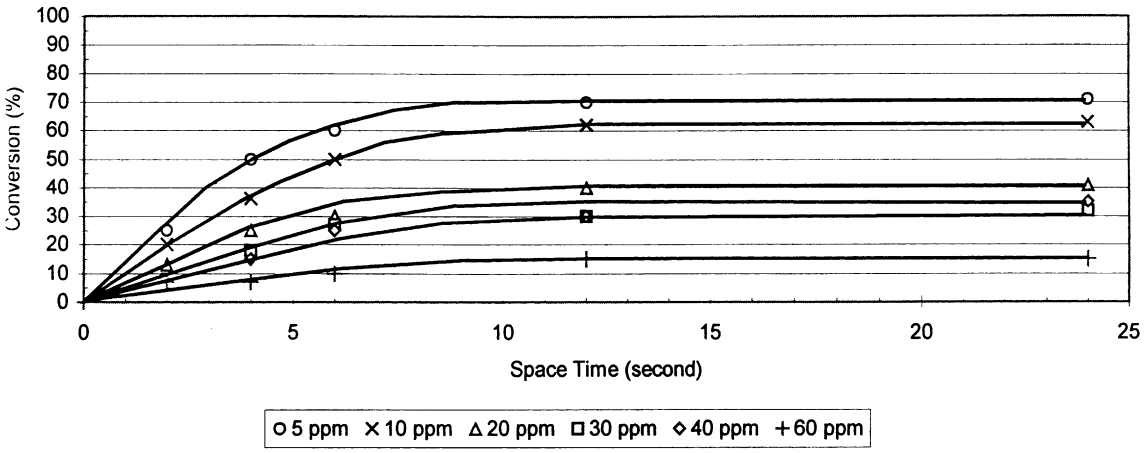

Fig. 4. Inlet concentration and space time effects.

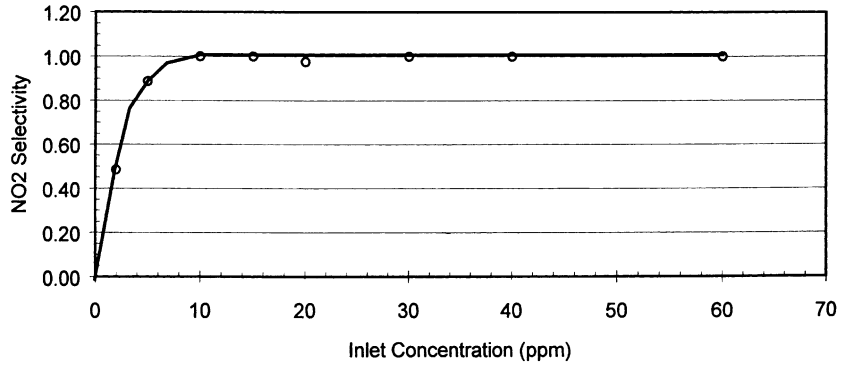

Fig. 5. NO_2 selectivity vs. inlet concentration (space time: 12 s, light source: 2 × 8 W BL, relative humidity: 50%, temperature: 74 °F, catalyst weight: ~1 mg/cm^2).

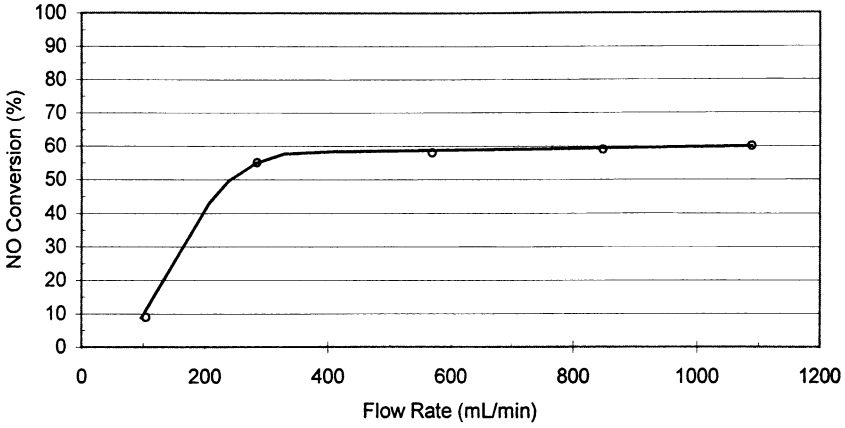

Fig. 6. NO conversion vs. gas flow rate at constant space time (9.2 s).

NO at the steady state, all NO should be converted to NO_2. We believe that for 5 ppm inlet NO the true steady state is not reached yet. Thus, increasing the light intensity dissociates HNO_3 back to NO_2 and $OH^\bullet$ and promotes the NO_2 selectivity from 82 to 95%.

3.4. Humidity effect

In this set of experiments, the percent of relative humidity (% RH) was varied from 0 to 75% at 25% increment with a 24 h irradiation time. The water concentration ranged from

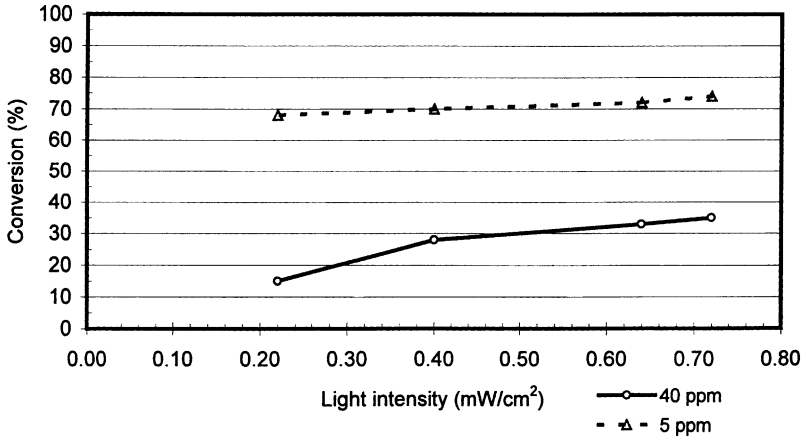

Fig. 7. NO_2 conversion vs. light intensity (space time: 12 s, inlet concentration: 5 and 40 ppm, relative humidity: 50%, temperature: 74 °F, catalyst weight: ~1 mg/cm^2, light source: 2 × 25 W BL with controller).

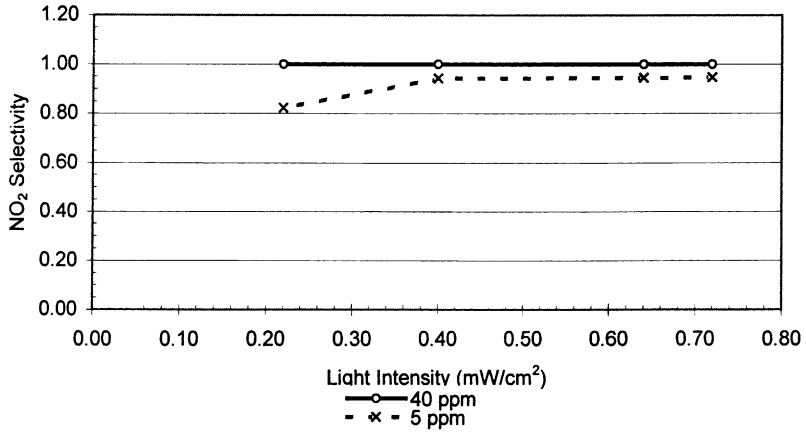

Fig. 8. NO_2 selectivity vs. light intensity (space time: 12 s, inlet concentration: 5 and 40 ppm, relative humidity: 50%, temperature: 74 °F, catalyst weight: ~1 mg/cm^2, light source: 2 × 25 W BL with controller).

0.12 to 870 mol/m^3. The other parameters were kept constant at the base condition: 40 ppm inlet concentration, 12 s space time, 74 °F, 2 × 8 W light source, and ~1 mg/cm^2 catalyst loading.

The conversion of NO increases from 0 to 50% RH and remains constant after 50% RH with a 24 h period of irradiation, Fig. 9. Since water is an essential contributor to $OH^{\bullet}$, it makes sense that increasing relative humidity enhances the NO conversion at the steady state. Note that the reactions take hours to reach a steady state; the TiO_2 surface that is initially hydroxylated thus needs to be replenished with water. NO_2 selectivity keeps constant at 100% at steady state for 40 ppm inlet concentration of NO over the entire RH range tested.

Tawara et al. [26] also carried out a similar experiment in which the gap between catalyst and wall was smaller (5 mm) and the inlet concentration was 1 ppm. As the relative humidity went higher than 50%, the conversion of NO decreased. This decrease may be due to the competitive adsorption between water and NO. As the NO concentration increases, NO has better chances to adsorb onto the catalyst surface as indicated in this study.

3.5. Nitrite and nitrate analysis

The liquor from washing the spent catalyst with deionized water was analyzed for NO_2^- and NO_3^- with an Alltech ion chromatograph as described in the experimental section. After 6 h of irradiation, the ratio of NO_2^- to NO_3^- from the spent-catalyst scrubbing liquor is steady, Fig. 10. The fact that nitrite and nitrate ions in the liquor are still not in equilibrium corroborates the observed transient behavior at the first few hours of operation. NO_3^- comes from HNO_3 [20] while nitrite comes from adsorbed HNO_2 (molecular

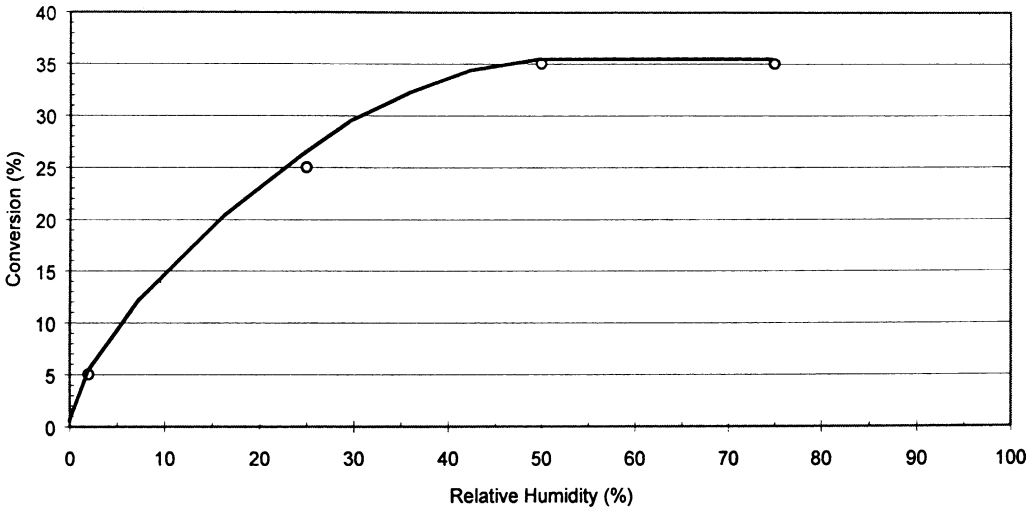

Fig. 9. Humidity effect on NO conversion (space time: 12 s, inlet concentration: 40 ppm, light source: 2 × 8 W BL, temperature: 74 °F, catalyst weight: ~1 mg/cm^2).

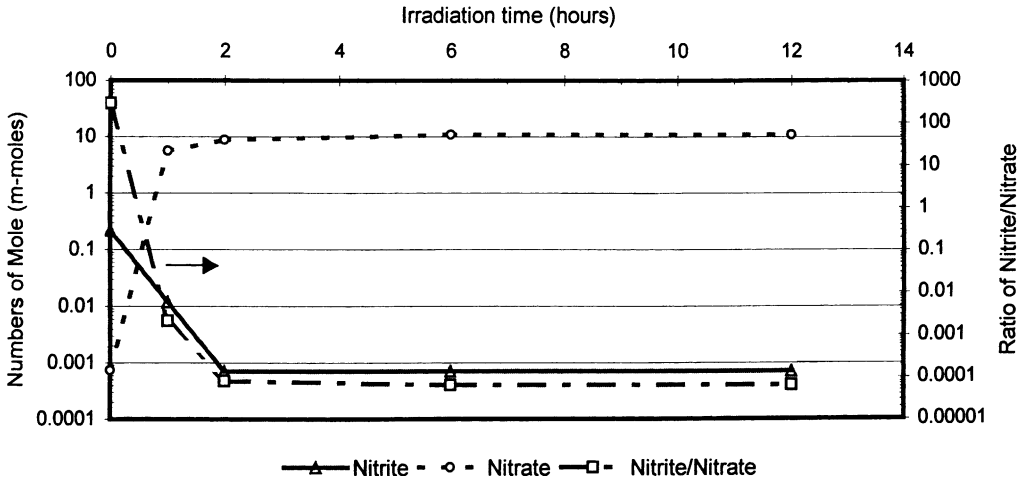

Fig. 10. Nitrite/nitrate ratio from spent catalyst scrubbing liquor vs. irradiation time.

and ion forms). It should be noted that HNO_2 is converted to NO (~90% efficiency) in the NO_x analyzer's molybdenum converter and reported as NO_2.

3.6. Reaction mechanism

The proposed reaction pathways are based on the products/intermediate species detected and the reaction data from literature and our laboratory. Homogeneous, atmospheric reactions rate constants involving hydroxyl/superoxide radicals and NO are abundant in the literature [27–30]. For example, k is reported to be in the order of $10^{-9}\,M^{-1}\,s^{-1}$ for OH with gas phase NO. Second-order rate constant k is $6.7 \times 10^{-9}\,M^{-1}\,s^{-1}$ for O_2^- reacting with NO in vivo. k is $3 \times 10^{-9}\,M^{-1}\,s^{-1}$ for OH reacting with gas phase NO_2. However, no rate constants are reported for heterogeneous photocatalytic reactions over TiO_2.

The photocatalytic oxidation of NO produces two major products: NO_2 gas and HNO_3 on catalyst surface. HNO_2 is a minor species on catalyst surface as seen in Fig. 10. As mentioned earlier, both HNO_3 and HNO_2 are produced in the initial/transient periods until the equilibrium between HNO_2, NO_2 and HNO_3 is established on the catalyst. When equilibrium is established, the feed NO is converted to NO_2 only. When a larger amount of catalyst is coated, a longer period of time is needed to reach a steady state. The key oxidant in this reaction is believed to be $OH^\bullet$ produced from water, O_2, and electron–hole pair on the catalyst surface.

When the UV light is first turned on, $OH^\bullet$ radical quickly reacts with adsorbed NO to form adsorbed HNO_2. At this point, the adsorbed HNO_2 can dissociate to H^+ and NO_2^-. Little NO can be desorbed, and NO_2 formation is slow as seen in the spike of nitrite, quick disappearance of NO, and the lack of gas phase NO_2, Figs. 2 and 10. This initial period only lasts about 0.5–3 min depending on the catalyst loading (0.7–2.9 mg/cm^2). Next, the formed HNO_2 further reacts with $OH^\bullet$ radical to generate adsorbed NO_2 and water. This second reaction gradually becomes competitive with the first reaction because the adsorbed NO becomes scarce (i.e. the active sites are occupied by more strongly adsorbed HNO_3 and HNO_2). The phenomenon can be seen in Fig. 10 where NO_2^- gradually decreases and NO_3^- gradually increases. The third reaction in series, i.e. NO_2 reacting with $OH^\bullet$ radical to form HNO_3, is always fast and eventually reaches equilibrium with its reverse reaction on the surface of the catalyst. The transient period is thus characterized with a series of oxidation steps: $NO \rightarrow HNO_2 \rightarrow NO_2 \rightarrow HNO_3$.

In Fig. 10, after 3 h, the amount of NO_2^- reaches a constant level. After 6 h, the amount of NO_3^- also reaches a constant level. It is believed that at the steady state and latter part of the transient period, the stable HNO_3 and its dissociated form (H^+ and NO_3^-) become dominant. Since the adsorbed HNO_3 dissociates to H^+ and NO_3^- to a great extent, the buildup of H^+ ion lowers the scrubbing liquor pH. The lower pH is responsible for the decrease of NO_2^- ion. As $[H^+]$ increases, the equilibrium shifts back to form HNO_2 and consumes NO_2^-. The labile HNO_2 will further undergo an oxidation or reduction reaction. The pH values of spent catalyst were measured by washing spent catalyst with 500 ml 18 MΩ water after different irradiation time. The pH value quickly goes down from 6.04 ± 0.07 to 4.85 after an initial irradiation and to 4.39 after 19 h irradiation [25].

At steady state, the equilibrium between HNO_3 and NO_2 is already reached on the catalyst surface. Once the catalyst is saturated with HNO_3, the oxidation reaction can only go as far as NO_2. At space time >12 s, a longer space time will not further increase the conversion of NO because the equilibrium has been established between all species on the catalyst surface including adsorbed NO, Fig. 4. The reaction regimes are described in Figs. 11 and 12. At the initial phase of the series reactions, NO is quickly adsorbed onto the catalyst and reacts with the hydroxyl radical to form nitrous acid (HNO_2). The adsorbed HNO_2 is in equilibrium with its dissociated ionic forms and can further react with

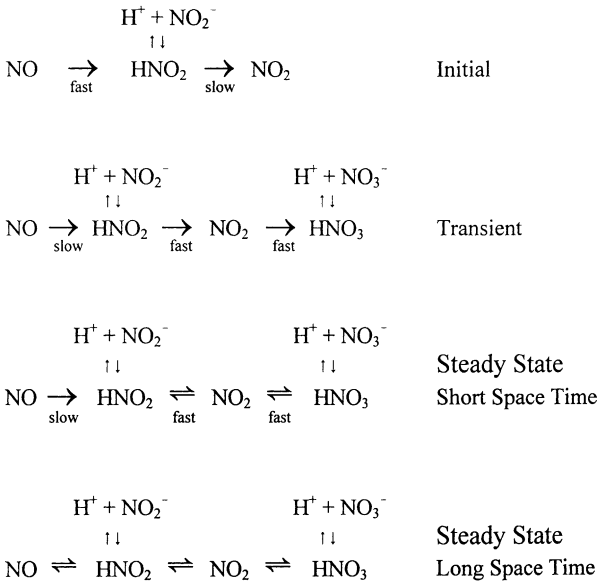

Fig. 11. Reaction regimes for photocatalytic oxidation of nitric oxide over TiO_2.

another hydroxyl radical to produce adsorbed NO_2. During the transient period, the adsorbed NO_2, which is in equilibrium with the gas phase NO_2, can be oxidized to produce HNO_3. The reaction mechanism of photocatalytic oxidation can also be presented in the networks shown in Fig. 12.

The following comments summarize the photocatalytic oxidation reactions of nitric oxide over TiO_2:

- At the initial stage, HNO_2 quickly accumulates, no NO_2 is observed.

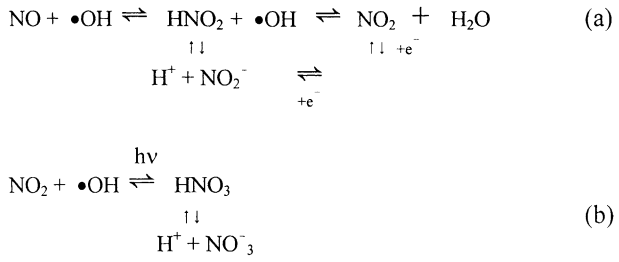

Fig. 12. Reaction networks for photocatalytic oxidation of nitric oxide over TiO_2.

- In the transient period, oxidation of HNO_2 to NO_2 and subsequent oxidation of NO_2 to HNO_3 take place.
- The stable HNO_3 and its dissociated ions become dominant at the latter transient period.
- At steady state, the oxidation reaction can only go as far as NO_2.
- With a long space time, equilibrium is virtually established for all fast reactions.

3.7. L–H model

The results from space time and inlet concentration effect studies were fitted into the L–H model. From the Marquardt nonlinear regression, the reaction constants and the adsorption equilibrium constants were determined. The L–H model is shown below:

$$-r_{NO} = \frac{K'_A C_{NO} C_{H_2O} - K'_B C_{NO_2}}{(1 + K'_{H_2O} C_{H_2O} + K'_{NO} C_{NO} + K'_{NO_2} C_{NO_2})^2} \quad (1)$$

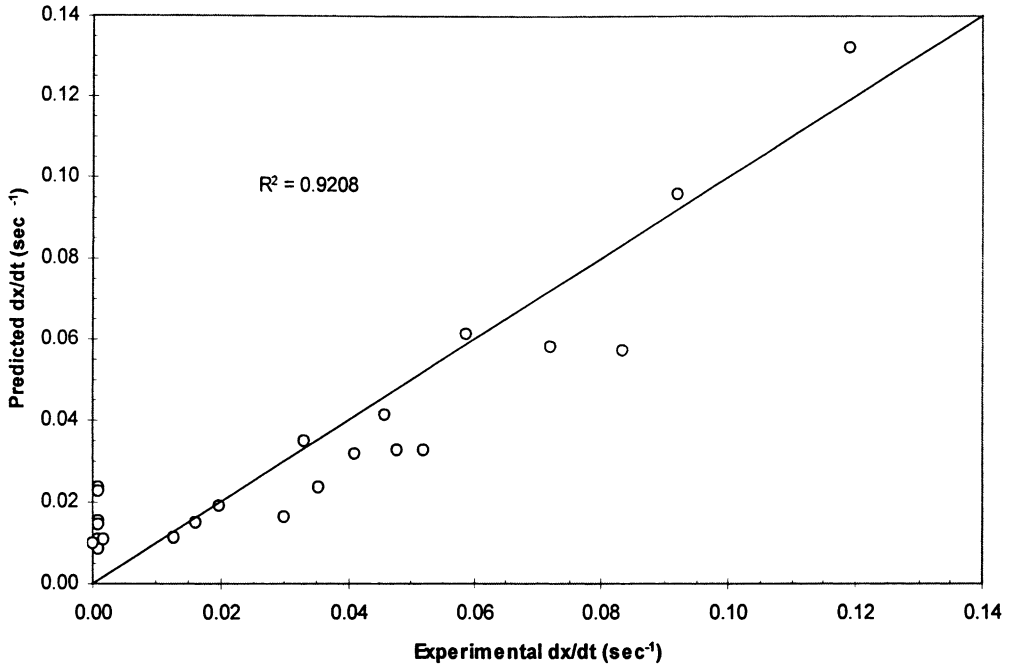

Fig. 13. Actual vs. predicted rates by the L–H model.

Table 1
Constants from nonlinear regression analysis

Constant	Estimate	Unit
K'_A	431.68 ± 179.46	m^3/(mol s g catalyst)
K'_B	81.84 ± 60.65	1/(s g catalyst)
K'_{H_2O}	43.55 ± 4.56	m^3/mol
K'_{NO}	$3.28 \times 10^4 \pm 2.06 \times 10^4$	m^3/mol
K'_{NO_2}	$9.04 \times 10^4 \pm 8.58 \times 10^4$	m^3/mol

where t is the space time (s); $-r_{NO} = -dC_{NO}/dt$ for a plug flow reactor; $-r_{NO}$ the disappearance rate of NO (mol/m^3 s); K'_A, K'_B the reaction rate constants; K'_{H_2O}, K'_{NO}, K'_{NO_2} the adsorption equilibrium constants; and C_{NO}, C_{NO_2}, C_{H_2O} the concentration of nitric oxide, nitrogen dioxide, and water in gas phase (mol/m^3).

The L–H model agrees very well with the experimental data (25 data points, $R^2 = 0.9208$), Fig. 13. The determined K'_A, K'_B, K'_{H_2O}, K'_{NO} and K'_{NO_2} are shown in Table 1. These constants are based on the room temperature data.

4. Conclusion

Photocatalytic oxidation of nitric oxide (NO), the major component of NO_x, yields nitric acid and nitrogen dioxide (NO_2). The latter can be collected in an adsorbent bed and then desorbed as NO_2 gas or hydrolyzed as nitric acid [21]. The treatment is a nitrogen fixation process and converts a pollutant into a raw material of fertilizer.

The thin-film photoreactor was irradiated with two 8 or 25 W black lights with an adjustable light intensity. The process involves a series of oxidation steps by the $OH^\bullet$ radical: $NO \rightarrow HNO_2 \rightarrow NO_2 \rightarrow HNO_3$. There is a pronounced transient period, typically lasting several hours. The amounts of NO_2^- and NO_3^- recovered from the catalyst change with irradiation time until a steady state is reached. The conversion increases with space time and decreases with inlet concentration. The reactions, however, are limited by thermodynamic equilibrium after ~12 s space time. Two 25 W black lights were used with a dimming electronic ballast to vary the light intensity. The light was measured with a radiometer in the range of 320–390 nm. Light intensity increases the capability to oxidize NO from 0 to 0.8 mW/cm^2. The NO_2 selectivity increases with light intensity for 5 ppm inlet NO but remains constant for 40 ppm inlet NO. The steady state NO conversion increases with relative humidity from 0 to 50% and then levels off at a higher relative humidity.

A photocatalytic oxidation mechanism is proposed in which hydroxyl ($OH^\bullet$) radical is a key oxidant in the PCO. The intermediate species, HNO_2, can be further oxidized to NO_2 and H_2O. The former is then oxidized to HNO_3, the major product deposited on the catalyst. The experimental data from space time and inlet concentration effects can be described with the L–H model with $R^2 = 0.9208$.

Acknowledgements

Financial supports from Texas Hazardous Waste Research Center (Grant #107LUB0698), Texas Higher Education Coordinating Board Advanced Technology Program (Grant #003581-0019-1999), and the Lamar University Research Enhancement Program are gratefully acknowledged.

References

[1] D. Elsom, Atmospheric Pollution, Basil Blackwell, New York, 1987.
[2] J.H. Seinfeld, S.N. Pandis, Atmospheric Chemistry and Physics: From Air Pollution to Climate Change, Wiley, New York, 1998.
[3] C.D. Cooper, F.C. Alley, Air Pollution Control: A Design Approach, Waveland Press, Prospect Heights, IL, 1994.
[4] US Environmental Protection Agency, Background Report AP-42, Nitric acid, Section 5.9, 1996. http://www.epa.gov.
[5] K. Patrick, Ultra-low NO_x burner has widened stability limits, 2000. http://www.chemicalonline.com.
[6] C.A. Latta, Plant Eng. 52 (10) (1998) 105–112.
[7] Chem. Eng. News 78 (35) (2000) 22.
[8] S.K. Gangwal, G.B. Howe, J.J. Spivey, P.L. Silveston, R.R. Hudgins, J.G. Metzinger, Environ. Prog. 12 (2) (1993) 128.
[9] K. Li, S.Y.C. Liu, S. Khetarpal, D.H. Chen, J. Adv. Oxid. Technol. 3 (3) (1998) 311.
[10] A. Fujishima, K. Hashimoto, T. Watanabe, TiO_2 Photocatalysis Fundamentals and Applications, BKC Inc., Tokyo, 1999.
[11] G. Munuera, et al., J. Chem. Soc., Faraday Trans. 75 (1979) 736.
[12] H. Gerischer, A. Heller, J. Phys. Chem. 95 (1991) 5261–5267.
[13] K. Li, S.Y.C. Liu, C. Huang, S. Esariyaumpai, D.H. Chen, J. Adv. Oxid. Technol. 5 (2) (2002) 227–232.
[14] http://www.nrel.gov/research/industrial_tech/pollution.html.
[15] R.D. Barreto, K.A. Gray, K. Anders, Water Resour. 29 (5) (1995) 1243–1248.
[16] S.R. Cater, B.W. Dussert, N. Megonnell, Pollut. Eng. 32 (5) (2000) 36–39.
[17] M. Anpo, Surface Science and Catalysis, vol. 130, Elsevier, Amsterdam, 2000, pp. 157–166.
[18] T. Ibusuki, K. Takeuchi, J. Mol. Catal. 88 (1994) 93–102.
[19] K. Suzuki, Photocatalytic air purification on TiO_2 coated honeycomb support, in: Proceedings of the First International Conference on TiO_2 Photocatalytic Purification of Water and Air, London, Ont., Canada, 8–13 November 1992.
[20] N. Negishi, K. Takeuchi, T. Ibusuki, Appl. Surf. Sci. 121/122 (1997) 417–420.
[21] D.H. Chen, et al., Photocatalytic oxidation of NO_x at source levels, in: Proceedings of the 1996 AIChE Annual Meeting, Chicago, IL, 10–15 November 1996.
[22] R.E. Kirk, D.F. Othmer (Eds.), Encyclopedia of Chemical Technology, 3rd ed., vol. 15, Wiley, New York, 1980.
[23] D.H. Kim, M.A. Anderson, W.A. Zeltner, J. Environ. Eng. August (1995) 590–594.
[24] S. Devahasdin, D.H. Chen, K. Li, Photocatalytic oxidation of nitric oxide to nitric acid, in: Proceedings of the Paper Presented at the 12th ICC Conference in Granada, Spain, 9–14 July 2000.
[25] C. Fan Jr., TiO_2-catalyzed photo-oxidation of NO_x, Master's Thesis, Lamar University, Beaumont, TX, 1997.

[26] H. Tawara, et al., Development of evaluation method of air-purifying paving blocks for NO_x removal capacity, in: Proceedings of the Fourth International Conference on TiO_2 Photocatalytic Purification and Treatment of Water and Air, Albuquerque, NM, 24–28 May 1999.
[27] http://allen.rad.nd.edu/icabr/RadChemHomePage.html.
[28] http://www.medicine.uiowa.edu/frrb/SRFRS/sunrisefreradschool99beckman.pdf.
[29] http://www.medicine.uiowa.edu/frrb/education/FreeRadicalSp01/Paper%201/AbdallaM-paper1.pdf.
[30] http://www.bioscience.org/1997/v2/d/jourd1/htmls/jourd.pdf.